MOLECULAR PHYSICS, 10 JANUARY 2004, VOL. 102, NO. 1, 37–45

Taylor & Francis
Taylor & Francis Group

Ab initio-based PES extrapolated using transferable atom–atom potentials, and predicted MW spectrum of the Ar–O_2($X\,^3\Sigma_g^-$) complex

F. Y. NAUMKIN[1]* and F. R. W. MCCOURT[2]†

[1]Department of Chemistry, University of Toronto, Toronto, Ontario M5S 3H6, Canada
[2]Department of Chemistry, University of Waterloo, Waterloo, Ontario N2L 3G1, Canada

(*Received 1 September 2003; revised version accepted 20 October 2003*)

A high-level *ab initio*-based ground-state Ar–O_2 potential energy surface has been obtained and employed to predict the microwave (MW) spectrum of the Ar–O_2 van der Waals complex. Transferability of the atom–atom components of the total interaction has been explored by extrapolating the original *ab initio* potential energy surface via accurate ArO and ArN potentials deduced from the rotational parameters of the Ar–NO and Ar–N_2 Van der Waals complexes. The extrapolated Ar–O_2 potential energy surface has then been tested by comparison with experimental Ar–O_2 scattering data. In addition, the extrapolated potential energy surfaces have been compared with other *ab initio*-derived and empirical atom–atom and atom–molecule potential energy surfaces in the literature.

1. Introduction

The Ar–O_2 system is a prototypical example of the interaction between a closed-shell atom and an open-shell molecule. Such species represent intermediates between closed-shell–closed-shell (exemplified by Ar–Ar) and open-shell–open-shell (typified by O_2–O_2) van der Waals interactions: they exhibit both first-order and second-order anisotropies. The first-order anisotropy originates from the sum of two-body (isotropic) components, and is characterized by a well associated with the T-shaped configuration. This anisotropy has been accounted for in a number of empirical ground-state Ar–O_2 potential energy surfaces (PESs) developed previously (see [1–3] and references therein) by fitting to experimental scattering cross-section data. These empirical potential functions (normally with two Legendre terms to represent the angular dependence) all give rise solely to a well for the T-shaped configuration. Early high-level *ab initio* calculations [4, 5] for the He–O_2 interaction had, however, revealed the existence of an additional (shallow) potential well for the linear configuration. This secondary well arises from a second-order anisotropy associated with the open-shell character of the atomic components of the molecule. A version of this relationship, which can already be seen from the simple atom–atom potential model of [6], has also been employed for other Ar–X_2 (X = carbon, halogen) interactions [7, 8].

The first high-level *ab initio*-based Ar–O_2 PES [6] utilized coupled-cluster supermolecule calculations of the interaction energies for the linear and T-shaped Ar–O_2 geometries and obtained interaction energies for other Ar–O_2 geometries by interpolation, using a model that employs *effective* ArO potentials. The parameters of the effective ArO potentials were determined by an appropriate scaling of initial high-level *ab initio* ArO($X^3\Pi$) and ArO($^3\Sigma^-$) potentials so that the model potential energy surface reproduced the high-level *ab initio* calculations for the two original cuts of the Ar–O_2 PES. Although the model PES exhibited two potential wells, with that for the linear configuration being shallower (as for the He–O_2 PES), it represented the interaction energies for intermediate bent geometries less accurately. We note that the double-well topology for the Ar–O_2 PES has also been confirmed by MP4 calculations [9] for four additional cuts (at $\theta = 20^\circ$, 40°, 60°, 80°) of the PES.

In the present work, a high-level *ab initio*-based Ar–O_2($X\,^3\Sigma_g^-$) PES has been constructed and has been employed to predict the microwave (MW) spectrum of the Ar–O_2 complex. Given the absence of experimental MW data for this complex, we have instead incorporated existing experimental data for the Ar–NO and Ar–N_2 complexes via extrapolated atom–atom potentials in the manner described below.

*Author for correspondence. e-mail: fnaumkin@utoronto.ca

Molecular Physics ISSN 0026–8976 print/ISSN 1362–3028 online © 2004 Taylor & Francis Ltd
http://www.tandf.co.uk/journals
DOI: 10.1080/00268970310001637944

The calculational procedures employed in determining the Ar–O_2 PES, and from it the MW spectrum of the Ar–O_2 van der Waals complex, are outlined in section 2. Section 3 contains the results of the present study and gives a discussion of their significance, while section 4 presents the conclusions to be drawn with regard to the reliability of the Ar–O_2 PES determined herein.

2. Calculational procedure

All ArO($X\,^3\Pi$, $^3\Sigma^-$) and Ar–O_2($X\,^3\Sigma_g^-$) energies have been calculated within the coupled-cluster RCCSD-T method [10, 11] (as implemented in the Molpro-98 program package [12]) using the spdf basis set *aug-cc-pVTZ* [13, 14], for both the ArO and Ar–O_2 complexes. In addition, the *spdfg* basis set *aug-cc-pVQZ* has been employed for the ArO calculations. All results have been corrected for basis-set superposition error in the standard manner [15].

The atom–atom model for the Ar–O_2 interaction is based upon the electronic structure of $O_2(X\,^3\Sigma_g^-)$, in which the π_x and π_y molecular orbitals are each singly occupied (the molecular axis defines the z direction). This model can be constructed readily from simple valence-bond considerations [6], or as a sum over the interactions between the Ar atom and the O_2 electrons [16]: the model can be written as

$$V^{\text{model}}_{\text{Ar–O}_2} = V_{\text{ArO}_a} + V_{\text{ArO}_b}, \tag{1}$$

in which the anisotropic ArO_i potentials are given in terms of the potentials $V_\Pi \equiv V(X^3\Pi)$ and $V_\Sigma \equiv V(^3\Sigma^-)$ by

$$V_{\text{ArO}_i} = V_\parallel(R_i)\cos^2\theta_i + V_\perp(R_i)\sin^2\theta_i, \quad i = a, b, \tag{2}$$

with $V_\parallel$ and $V_\perp$ defined by

$$V_\parallel = V_\Pi, \quad V_\perp = \tfrac{1}{2}(V_\Pi + V_\Sigma). \tag{3}$$

This model, represented by equations (1)–(3), is similar to that for the Ar–B_2 [16] interaction because of its analogous electronic structure. The position of the Ar atom relative to the O atom i in the O_2 molecule is given by the polar coordinates (R_i, θ_i).

More accurate ArO data (designated by $V^{\text{new}}_{\text{ArO}}$) can be incorporated into the model Ar–O_2 potential by transferring the difference between the *ab initio* Ar–O_2 PES (designated by $V_{\text{Ar–O}_2}$) and the model-predicted PES with *ab initio* ArO input, both calculated at a given level of theory, to the model PES with the more accurate ArO input. This procedure allows a correspondingly more accurate Ar–O_2 PES to be constructed. The appropriate equation for accomplishing this is

$$\begin{aligned} V^{\text{new}}_{\text{Ar–O}_2} &= (V^{\text{new}}_{\text{ArO}_a} + V^{\text{new}}_{\text{ArO}_b}) + [V_{\text{Ar–O}_2} - (V_{\text{ArO}_a} + V_{\text{ArO}_b})] \\ &= V_{\text{Ar–O}_2} + \Delta^{\text{model}}, \end{aligned} \tag{4}$$

in which Δ^{model} is given by

$$\Delta^{\text{model}} = (V^{\text{new}}_{\text{ArO}_a} + V^{\text{new}}_{\text{ArO}_b}) - (V_{\text{ArO}_a} + V_{\text{ArO}_b}). \tag{5}$$

The more accurate ArO potentials can be obtained either from still higher-level *ab initio* calculations or from empirical sources.

Employment of this extrapolation procedure to determine the $ArCl_2$ (or $NeCl_2$) interaction PES using *ab initio* ArCl (NeCl) potentials of higher accuracy or empirical ones has been shown [8, 17] to reproduce the corresponding higher-level *ab initio* or (in terms of parameters) experimental triatomic PES rather well.

Rotational parameters have been calculated using the TRIATOM program package [18], with pre-optimized extensive basis sets of Morse eigenfunctions for the radial and Legendre polynomials for the angular dependences, while scattering cross-sections have been evaluated within the infinite-order sudden (IOS) approximation.

3. Results and discussion

The Ar–O_2 PES has been calculated for twelve R values at each of five equidistant values of θ between 0° and 90°, where (R, θ) are the polar coordinates of the Ar atom relative to the centre of mass of the O_2 molecule fixed at its ground-state equilibrium interatomic distance, $r_e = 1.21$ Å. The PES has two wells, with that for the linear configuration being somewhat shallower than that for the T-shaped configuration (see figure 1). Interpretation of this topology in terms of the atom–atom model (1)–(3) is straightforward: the interaction between Ar and O in O_2 is determined by $V_\parallel = V_\Pi$ and (mainly) $V_\perp = 1/2(V_\Pi + V_\Sigma)$ in the linear and T-shaped geometries, respectively. Deviation of the Ar atom from the linear geometry increases the contribution from the less attractive $V_\perp$, thereby reducing the binding. This explains the well for the linear configuration. The lower stability of this well for the *ab initio* PES as compared to the model PES with the *ab initio* ArO input of the same accuracy (figure 2) can be associated with *sp*-hybridization of the O orbitals within O_2, similar to other Ar–X_2 (X = N, C, B) cases [19, 7, 16]. For the T-shaped geometry, the Ar–O_2 interaction is dominated by $2V_\perp$, which is more attractive than $V_\parallel$ between Ar and the nearest O, dominating in the linear geometry. This explains the relative depths of the two wells.

The equilibrium parameters for the various Ar–O_2 ($X^3\Sigma^-$) PESs under discussion are collected in table 1. The binding energies for the two geometries obtained

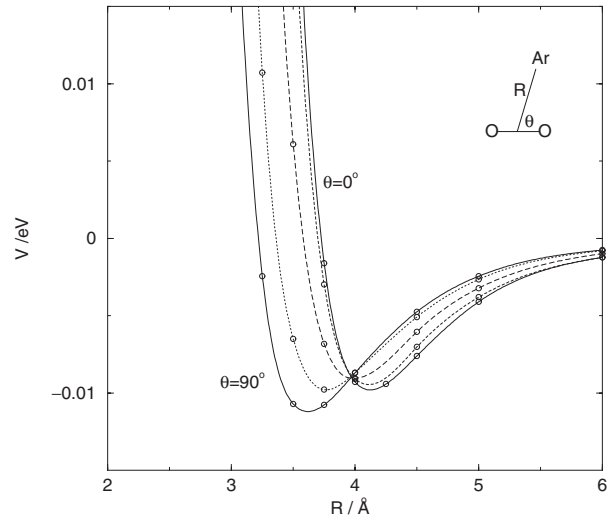

Figure 1. Radial cuts of the Ar–O_2($X\,^3\Sigma_g^-$) PES (from right to left – at $\theta = 0°, 22.5°, 45°, 67.5°, 90°$): *ab initio* (RCCSD-T/*spdf*) data interpolated with cubic spline curves.

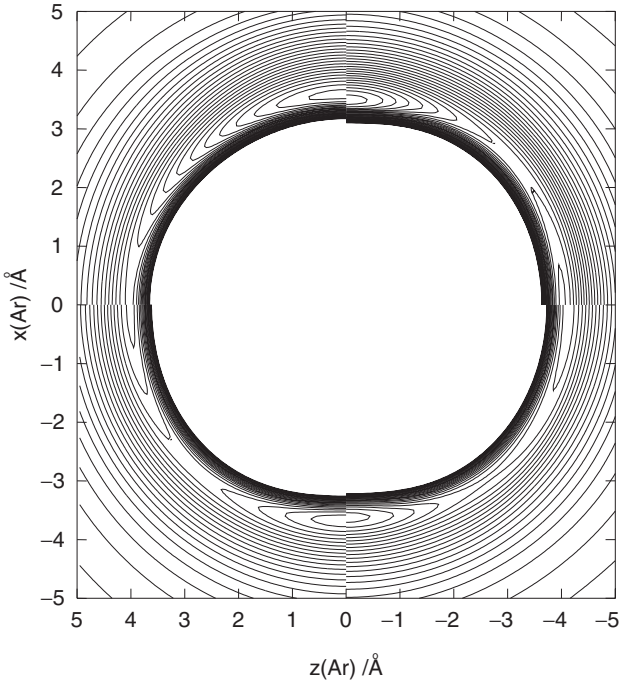

Figure 2. Contour maps of the Ar–O_2($X\,^3\Sigma_g^-$) PES: empirical [3] (upper left), atom–atom model (lower left), *ab initio* (lower right), extrapolated (upper right). x and z are the coordinates of Ar relative to the centre of O_2 fixed along the z axis. The contour step is 0.5 meV.

from the RCCSD–T/*spdf* coupled-cluster calculations differ by about 10 cm^{-1} at the equilibrium distances, which are 0.5 Å apart. The atom–atom model reproduces the *ab initio* D_e and R_e values within 3 cm^{-1} and 0.1 Å, respectively; however, the deviation from the D_e value for the linear configuration has the opposite sign to the deviation from the D_e value for the T-shaped configuration. Comparison with recent UMP4 calculations [9] shows that the addition of bond functions (*bf*) to the basis set increases the D_e values by about 30% and shortens the R_e values by about 0.1 Å for both configurations. These changes agree well with the predictions of the atom–atom model using equivalently accurate ArO potentials (i.e. RCCSD-T/*spdf* and UMP4/*spdf*+*bf* [20]): indeed, as can be seen from table 2, V_Π and V_Σ obtained from the UMP4 calculations are about 30% deeper and the R_e values are about 0.1 Å shorter than the corresponding RCCSD-T values. The UMP4 Ar–O_2 PES is also more attractive than the empirical potential surfaces [2, 3] obtained by fitting to crossed molecular beam scattering data. While there is only a small difference between the depths of the wells for the T-shaped configuration, there is a profound difference between these surfaces for the linear configuration, as the empirical surfaces have, by construction, only a saddle point there (figure 2). The corresponding UMP4 and empirical equilibrium distances lie within 1% of one another for both geometries. This behaviour is consistent with a previous *ab initio* study [24] of the He–Cl_2 system, where a relatively weak sensitivity of the scattering cross-sections to the potential well depth was obtained for fixed R_e, and the main contribution to the scattering cross-section came from the T-shaped geometry.

The present PES can be improved further by incorporating more accurate ArO potentials via equation (4). The empirical ArO potentials [21] obtained by fitting potential parameters to crossed molecular beam scattering data can be seen from table 2 to be less attractive than the corresponding *ab initio* potentials calculated at the UMP4/*spdf*+*bf* level: this is apparent particularly from the significantly shorter *ab initio* values for R_e. Moreover, for these *ab initio* R_e values more accurate single-point energy calculations [20] at the CCSD-T/*spdfg*+*bf* level give D_e values that exceed those for the empirical potentials for both ArO states.

Table 1. Equilibrium parameters (in cm^{-1} and Å) of the Ar–O_2 ($X\,^3\Sigma_g^-$) PES.

	Linear ($C_{\infty v}$)		T-shaped (C_{2v})	
	D_e	R_e	D_e	R_e
Empirical (scattering) [2]	{77.1}	4.00	113.5	3.56
Empirical (scattering) [3]	{69.8}	4.0	114.7	3.58
UMP4/*spdf* + *bf* [9]	103.8	4.0	117	3.55
RCCSD-T/*spdf*	79.1	4.12	90.4	3.62
atom–atom model (1)–(3)[a]	82.2	4.01	87.2	3.67
Extrapolated[b] via equation (4)	101.8	4.01	127.4	3.48

{}mark saddle points.
[a]With RCCSD-T/*spdf* ArO input.
[b]Using the scaled ArO potentials deduced from fitting R_0 for Ar–NO.

Table 2. Equilibrium parameters (in cm^{-1} and Å) of the ArO potentials.

	$X^3\Pi$		$^3\Sigma^-$	
	D_e	R_e	D_e	R_e
Empirical (scattering) [21]	83.9	3.45	41.2	3.85
QZQC [22] (BSSE-corrected)	62.1	3.46	35.6	3.88
UMP2/*spdf* + *bf* [20]	72.8	3.42	39.9	3.86
UMP4/*spdf* + *bf* [20]	83.7	3.38	48.2	3.80
UCCSD(T)/*spdfg* + *bf* [20]	≥85.5[a]		≥48.2[a]	
RCCSD-T/*spdf* [6]	64.5	3.45	34.9	3.89
RCCSD-T/*spdfg* [6]	75.8	3.39	42.1	3.84
exp-extrapolated, equation (6)	84.1	3.34	45.9	3.83
diexp-extrapolated, equation (7)	83.2	3.35	46.5	3.82
n^{-3}-extrapolated, equation (8)	85.1	3.35	47.7	3.81
Scaled[b] via equation (9)	89.7	3.33	50.3	3.80

[a]Single-point calculations at R_e (UMP4/*spdf* + *bf*).
[b]Fitting the R_0 value [23] of Ar–NO.

As is to be expected, these observations on the ArO potentials are also in accord with the results already discussed for the Ar–O_2 interaction.

As binding energies consistently increase with accuracy, it appears to be reasonable to extrapolate the ArO potentials to a basis-set limit. Three extrapolation schemes [25–27] commonly employed to obtain the basis-set limit are the exponential (*exp*), double-exponential (*diexp*), and reciprocal-power (n^{-3}) schemes given, respectively, by

$$V_n = V_\infty + A\exp(-Bn), \tag{6}$$

$$V_n = V_\infty + A\exp(-[n-1]) + B\exp(-[n-1]^2), \tag{7}$$

$$V_n = V_\infty + A/n^3, \tag{8}$$

in which $n = 2, 3, 4$ for D,T,Q in the aug-cc-PVnZ series of basis sets used to calculate the potentials V_n, and (the limit) V_∞, A and B are fitting parameters. Not surprisingly, the RCCSD-T/*spdfg* potentials are bound more strongly than the *spdf*-based potentials, but more weakly than the UMP4/*spdf*+*bf* versions (see table 2). The results of these three extrapolations are similar, with D_e and R_e varying within $2\,cm^{-1}$ and 0.02 Å, respectively. The most attractive n^{-3}-extrapolated potentials are only marginally (within $0.5\,cm^{-1}$) less deep than those directly calculated [20] with bond functions at single points. The results of such basis-set limit extrapolations will thus be different when bond functions are included, and may therefore depend somewhat on the particular *ab initio* method and basis sets employed for the calculations. Moreover, the R_e values for the extrapolated potentials are slightly (within 0.03 Å) longer (V_Σ) or shorter (V_Π) than those calculated directly using the UMP4/*spdf*+*bf* scheme. As we wish to predict a reliable microwave (MW) spectrum both for eventual comparison with experiment and to aid experimentalists in locating individual MW lines, a further attempt to try to improve the accuracy of V_{ArO} is justified.

Rather than attempting to extrapolate the ArO potentials to the basis-set limit, we can obtain them by fitting appropriate rotational parameters of an Ar complex with another O-containing molecule, XO, directly via an analogue of equation (4). To do this consistently, we need to have at our disposal both the Ar–XO PES and the ArX potentials, all calculated at the same level of theory. For instance, we can fit the experimental (vibrationally averaged) R_0 value of the Ar–NO complex [23], using its RCCSD-T/*spdf* PES [28] and the matching ArN potential [19]. However, we also need a reliable rotationally-based empirical ArN potential: while such a potential is, to the best of our knowledge, currently unavailable, it can be generated by carrying out a similar fitting of the experimental frequencies of the MW spectral lines for the Ar–N_2 complex [29], using its CCSD-T/*spdf* PES [19]. These subsequent steps are carried out below.

A method for extrapolating the *ab initio* ArX potentials beyond equations (6)–(8) is to scale them linearly via the relation

$$V_{ArX}^{new} = V_{ArX}^{spdf} + f(V_{ArX}^{spdfg} - V_{ArX}^{spdf}) = (1-f)V_{ArX}^{spdf} + fV_{ArX}^{spdfg} \tag{9}$$

using a scaling factor $f > 1$. This scaling preserves the trend in the variation of the potentials imposed by the *ab initio* data, i.e. that binding usually increases with increased accuracy. This differs from an unconditional optimization of the fitting parameters of an analytic representation in which preservation of the *ab initio*-based trend is not assured. It would also be possible to scale the correlation energy: this type of scaling has produced much the same result as an extrapolation having the form of equation (9) for the ArB interaction [16].

For the Ar–$N_2(X\,^1\Sigma_g^+)$ complex the experimental $1_{01}-0_{00}$ transition frequency ν_1 has been reproduced accurately using the PES obtained from equation (4) (with 'O' replaced by 'N' and an isotropic V_{ArN}) with $f = 1.85$ in equation (9). The resultant PES is 10–15% deeper than the original *ab initio* PES [19] obtained with the *spdfg* basis set, and it has an R_e value that is shorter by 0.05 Å (see table 3). The global minimum is slightly deeper, by $2\,cm^{-1}$, and lies closer to the origin, by 0.02 Å, than for the analytically-fitted CCSD(T)/*spdf*+*bf* PES [30], and is very close (within $1\,cm^{-1}$ in

Table 3. Equilibrium parameters (in cm^{-1} and Å) of the $Ar–N_2(X^1\ \Sigma_g+)$ PES.

	Linear ($C_{\infty v}$)		T-shaped (C_{2v})	
	D_e	R_e	D_e	R_e
CCSD(T)/*spdf* + *bf* (fit) [30]	{75.3}	4.27	99.1	3.72
Scaled CCSD(T) fit [30]	{78.0}	4.24	101.6	3.70
CCSD-T/*spdf* [19]	{64.0}	4.33	81.0	3.80
CCSD-T/*spdfg* [19]	{70.0}	4.29	89.1	3.75
Extrapolated via equation (4)[a]	{77.0}	4.25	100.5	3.70

{}mark saddle points.
[a]With O replaced by N.

D_e and <0.01 Å in R_e) to the scaled version of this PES fitted to the same experimental MW data. Moreover, the present extrapolated PES leads to a D_0 value, 79.7 cm^{-1}, which is identical to the value obtained with the MW-fitted PES [30].

The remaining minor differences between the current extrapolated Ar–N_2 PES and that of [30] can be associated both with limitations of the present extrapolation procedure and with the prediction [30] that the Ar–N_2 binding energy decreases slightly with basis-set extension when bond functions are included. The prediction of a decrease in well depth differs from increases predicted both in the absence of bond functions and with further scaling [30] to reproduce the MW data. It seems probable that a similar scaling would also produce a slightly shallower Ar–O_2 PES if the starting point were an *ab initio* PES obtained for the larger basis set, including bond functions (i.e. *spdfg* + *bf* [30]).

The corresponding scaled ArN($X^3\Sigma^-$) potential from equation (9) has $D_e = 67.9\ cm^{-1}$ ($R_e = 3.63$ Å), which should be compared to the values of 60.8 cm^{-1} (3.68 Å) and 53.4 cm^{-1} (3.73 Å) obtained for the RCCSD-T/spdfg and /*spdf* versions of the potential. These predicted equilibrium parameters for V_{ArN}^{new} are consistent with the values $D_e = 64.7$, 65.5, 66.8 cm^{-1} (all for $R_e = 3.64$ Å) obtained from the basis-set limit extrapolations of equations (6)–(8), with the scaled potential obtained from equation (9) being slightly more attractive. As can be seen from table 2, this is in accord with the relation between the results of similar basis-set limit extrapolations and the most accurate direct *ab initio* (UCCSD(T)/*spdfg* + *bf*) data for ArO. The ArN potential produced in this manner thus appears to be highly accurate. Unfortunately, there appears to be no empirical ground-state ArN potential available for comparison.

We can now employ this ArN potential in the analogue of equation (4) (i.e. with one of the O atoms replaced by an N atom) for the Ar–NO complex to fit its experimental R_0 value by scaling the ArO potentials via equation (9). Ground state NO($X^2\Pi$) is an open-shell molecule with one singly occupied π-orbital whose two possible orientations relative to the Ar–NO plane generate two PESs, one with A′ symmetry, the other with A″ symmetry. Due to the relative weakness of the interaction they are close enough in energy that the spin–orbit coupling in NO mixes them efficiently to produce two nearly equidistant relativistic Ar–NO($X\,^2\Pi_{1/2}$, $^2\Pi_{3/2}$) PESs [28], separated approximately by the value of the spin–orbit splitting Δ of the NO molecule. Since Δ (which is approximately 120 cm^{-1}) is significantly larger than the zero-point energy (which is approximately 30 cm^{-1} [31]), the ground-state relativistic PES can be treated independently for the evaluation of its lowest rovibrational states.

This PES is given by [32]

$$V_{Ar-NO(X)} = \frac{1}{2}\left[V_{A'} + V_{A''} - [(V_{A'} - V_{A''})^2 + \Delta^2]^{1/2}\right]. \quad (10)$$

The associated atom–atom model is given as $V_{A',A''}^{model} = V_{ArN} + V_{ArO(A',A'')}$, in which $V_{ArO(A'')} = V_\Pi$ and $V_{ArO(A')}$ is given by equation (2), with $V_\parallel = V_\Pi$ and $V_\perp = V_\Sigma$ [28].

The ArO potentials for both the $X\,^3\Pi$ and $^3\Sigma^-$ states have been scaled via equation (9) with the same value $f = 2.06$ for the scaling factor: this scaling factor allows accurate reproduction of the experimental value [23] $R_0 = 3.711$ Å for the Ar–NO complex. This value for f is somewhat larger than that obtained for ArN ($f = 1.85$): this may perhaps be anticipated for calculations using the same *ab initio* method and the same basis-set size for a system with an additional electron, thereby requiring a (slightly) larger correction.

The extrapolated Ar–NO(X) PES is more attractive (with D_e approximately 20–30 cm^{-1} larger and R_e approximately 0.1 Å shorter) than the original RCCSD-T/spdf PES (see table 4). The associated D_0 value is found to be 10 cm^{-1} larger than that for the recent PES *diexp*-extrapolated to the basis set limit in terms of UCCSD-T/*spdf* and /*spdfg* data [31] (giving rise to a value of R_0 somewhat in excess of the experimental value). This is consistent with a slight underestimation of the binding energy by *diexp*-extrapolated ArO potentials (table 2), and with their ArN counterparts being slightly less attractive than the ArN potentials scaled to fit the Ar–N_2 microwave data. The present predicted value $D_0 = 93.2\ cm^{-1}$ for Ar–NO is very close to the previously anticipated [35] value of approximately 95 cm^{-1} and falls within the rather wide experimental interval of 88–120 cm^{-1} [33, 34, 36].

As can be seen from the final entries in columns 2 and 4 of table 2, and as shown in figure 3, the current scaled ArO potentials are consistent with the lower bounds for the binding energies obtained for these two states [20] at the UCCSD-T/*spdfg* + *bf* level, and are slightly more

Table 4. Equilibrium parameters (in cm^{-1} and Å) of the ground state Ar–NO($X^2\ \Pi_{1/2}$) PES.

	$(C_{\infty v})$(N end)		C_s (Well)				$(C_{\infty v})$(O end)	
	D_e	R_e	D_e	R_e	D_0	R_0	D_e	R_e
diexp-extrapolated UCCSD(T) [31]					83.2	3.772		
RCCSD-T/*spdf* [28]	71.4	4.32	90.9	3.68			74.3	4.10
Extrapolated via equation (10)[a]/R_0-fit	88.5	4.23	122.6	3.56	93.2	3.711	94.8	4.00
Experiment [36]					87.8			
Experiment [33, 34]					105 ± 15			
Experiment [23]						3.711		

[a]Using $V^{new}_{A',A''} = V_{A',A''} + [V^{new}_{ArN} + V^{new}_{ArO(A',A'')}] - [V_{ArN} + V_{ArO(A',A'')}]$.

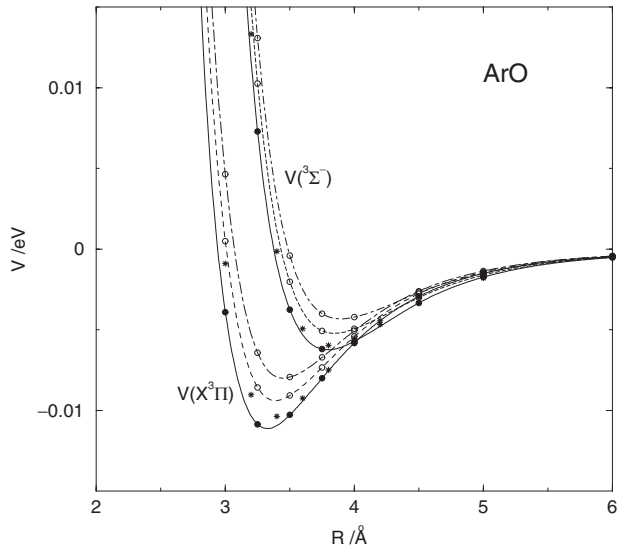

Figure 3. The ArO($X^3\Pi$, $^3\Sigma^-$) potentials: present *ab initio* (RCCSD-T/{*spdf* and *spdfg*}) and extrapolated data cubic-splined with dot-dashed, dotted and solid curves, respectively; UMP4/*spdf*+*bf* [20] points (∗).

attractive than the n^{-3}-extrapolated and UMP4/*spdf*+*bf* potentials. They appear to be highly accurate, much as we have noted for similar potentials obtained for the ArN complex, and discussed in detail in previous paragraphs. Their reliablility is further confirmed by the following observations. Inclusion of spin–orbit coupling preserves the relative binding of the ArO potentials calculated at different levels of theory. The increase of binding from the UMP2 to UMP4 potentials (see table 2) has been shown [20] to provide better agreement with the experimental Ar–O scattering data, although the cross-sections are still somewhat underestimated. The slightly increased attraction of the present scaled potentials could therefore further improve the comparison with the scattering data. This can be attributed to the *ab initio*-based ArO potentials (integrated over coordinate space) being closer to the empirical potentials (which have shallower wells at greater distances) which have been fitted directly to the experimental cross-sections. This simply reflects the possibility of having multiple equivalently accurate potential fits to a limited set of experimental data.

Use of the present scaled ArO potentials in equation (4) produces an Ar–O_2 PES which is 30–40% deeper than its RCCSD-T/spdf precursor and slightly more attractive (with D_e 10 cm^{-1} greater, and R_e 0.07 Å shorter for the T-shaped configuration) than the UMP4/*spdf*+*bf* PES (see table 1). Such an increase in the binding energy is consistent with what has been found for the Ar–N_2 and Ar–NO interactions.

For an additional check of its quality, the final PES has been employed to calculate the Ar–O_2 scattering cross-section for comparison with the cross-section obtained using the empirical PES [3] fitted directly to the experimental scattering data. As can be seen from figure 4, the scattering cross-section calculated from the extrapolated PES approximates the experimental cross-section rather well, especially at larger scattering angles. Moreover, it shows considerable improvement over the results obtained from the original RCCSD-T/*spdf* PES. The UMP4/*spdf*+*bf* PES [9] performs somewhat better than the extrapolated PES for small scattering angles ϕ, performs comparably accurately in the neighbourhood of the maximum (which occurs at $\phi = 7°$), but leads to a systematic overestimation of the experimental data for $\phi > 15°$. As the present extrapolated PES has been generated with no reference to the scattering experiments, its performance can thus be considered to be rather good. This comparison further illustrates the possibility of comparably accurate fits being obtained with two PESs of rather different topologies (*cf.* the two upper panels of figure 2).

Finally, the new (extrapolated) PES has been employed to predict the bond energy for and MW spectrum of the $^{40}Ar-^{16}O_2$ van der Waals complex. The calculated $v = 0$ rotational energy levels for $J = 1$, 2, 3, and the associated transition frequencies are presented in table 5. As the nuclear spin of the ^{16}O atom is zero, only rotational states of $^{16}O_2(X\,^3\Sigma_g^-)$ with odd j can exist [37]. The J_{0J} rotational states are thus forbidden for the

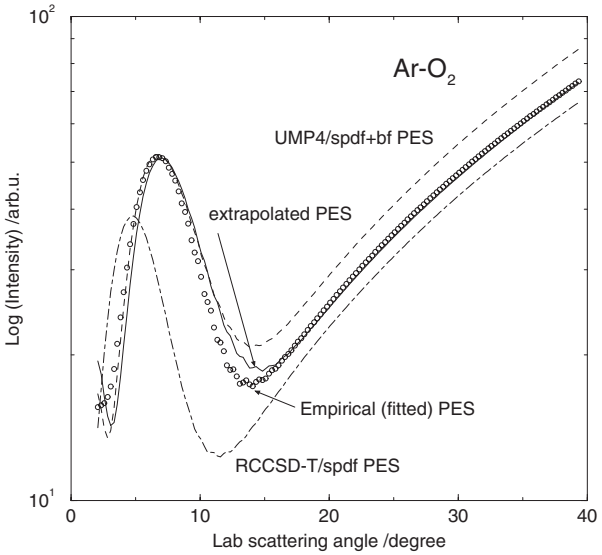

Figure 4. The Ar–O_2 differential scattering cross-sections from different potential surfaces: empirical PES [2] (○); present *ab initio* (RCCSD-T/*spdf*) PES and extrapolated PES (dot-dashed and solid curves, respectively); UMP4/*spdf*+*bf* [9] (dashed curve).

Table 5. Rotational levels (in cm^{-1}) and transition frequencies (in GHz) of $^{40}Ar-{}^{16}O_2$ ($v = 0$).

$J_{K_aK_c}$	E^a	$J'_{K'_aK'_c} - J''_{K''_aK''_c}$	ν
(0_{00})	0.0		
(1_{01})	(0.141)	$(1_{01}-0_{00})$	(4.235)
(2_{02})	(0.424)	$(2_{02}-1_{01})$	(8.469)
(3_{03})	(0.847)	$(3_{03}-2_{02})$	(12.700)
1_{11}	1.644		
2_{12}	1.922	$2_{12}-1_{11}$	8.323
3_{13}	2.338	$3_{13}-2_{12}$	12.482
1_{10}	1.649		
2_{11}	1.935	$2_{11}-1_{10}$	8.589
3_{12}	2.365	$3_{12}-2_{11}$	12.880

[a]Relative to the ground rovibrational state at $-95.811\,cm^{-1}$.
Brackets mark rotational states and transitions forbidden in terms of nuclear spin considerations for $^{16}O_2$.

^{40}Ar–$^{16}O_2$ complex [38], 0_{00} in particular, and consequently D_0 must be relative to the 1_{11} level, which lies $1.6\,cm^{-1}$ higher in energy. The predicted D_0 value (which is associated with the T-shaped conformer) of $95.8\,cm^{-1}$ corresponding to the 0_{00} state should then be replaced by $94.2\,cm^{-1}$. Both values are close to the D_0 value for Ar–NO and exceed the UMP4/*spdf*+*bf* value of $88.1\,cm^{-1}$ [9], in accord with the difference between the corresponding values of D_e. The ground rovibrational state energy level lies just above the barrier ($-96.4\,cm^{-1}$ relative to Ar + O_2 and located at $R_m = 3.93$ Å, $\theta_m = 38.8°$) separating the two wells. This is similar to the result for the UMP4/*spdf*+*bf* PES [9] PES, which has a barrier energy $-90.3\,cm^{-1}$, as obtained from their analytical fit.

The nuclear-spin considerations discussed in the previous paragraph imply that the MW spectrum for ^{40}Ar–$^{16}O_2$ will consist of a set of doublets rather than of the triplets of closely spaced lines that usually characterize a T-shaped complex. This happens because transitions between the J_{0J} levels of ^{40}Ar–$^{16}O_2$ cannot be seen, and only the J_{1J} and $J_{1\,J-1}$ components of the MW spectrum remain visible. The same applies to ^{40}Ar–$^{18}O_2$, as ^{18}O has zero nuclear spin as well. For Ar–O_2 van der Waals complexes involving the ^{17}O isotopomer (which has nuclear spin 5/2), the MW spectrum will include the J_{0J} component, so that the MW spectrum for the ^{40}Ar–$^{17}O_2$ complex consists of the usual triplets of lines. It would be encouraging and useful for fine tuning of the PES were an experimental MW spectrum available for comparison with the predictions given in table 5.

4. Conclusions

A high-level *ab initio* ground-state PES that exhibits the usual (two-body) well for the T-shaped configuration plus a shallower well for the linear configuration has been obtained for the Ar–O_2($X^3\Sigma_g^-$) interaction. This double-well topology is readily interpreted, and can be reproduced accurately (including well depths to within a few cm^{-1}), by a simple model which utilizes anisotropic atom–atom interactions based on the O_2 electronic structure and employs accurate *ab initio* ArO potentials as input.

In order to make a reliable prediction of the MW spectrum of the $^{40}Ar^{16}O_2$ van der Waals complex, the PES has been extrapolated by incorporating, via the anisotropic atom–atom model, more accurate ArO potentials. These potentials have been obtained by scaling high-level *ab initio* ArO potentials incorporated into the analogous atom–atom model for the Ar–NO van der Waals complex and by fitting to the experimental value of R_0 obtained for this complex. The corresponding ArN input potential has, in turn, been obtained by using a similar procedure in which the lowest-frequency MW line of the Ar–N_2 van der Waals complex has been fitted. The general sequence of transferring these atom–atom potentials can thus be summarized by the representation Ar–N_2 → ArN → Ar–NO → ArO → Ar–O_2. The ArN and ArO potentials scaled in this manner are consistent with other *ab initio* results (for ArO) and commonly-employed basis-set-limit extrapolations (particularly that using n^{-3}). Similarly, the corresponding extrapolated Ar–N_2, Ar–NO and Ar–O_2 PESs are consistent with other scaled *ab initio* results for Ar–N_2 and Ar–NO. In particular, we note that the Ar–N_2 PES extrapolated according to equation (4), and discussed

in the previous section, is almost identical to the final scaled *ab initio* PES of Fernandez *et al*. [30] that was fitted directly to the same MW data.

The present Ar–O_2 PES has been shown to provide an accurate description of the experimental molecular beam scattering cross-sections, and gives rise to an MW spectrum that is non-typical of a T-shaped complex in being composed of doublets, rather than triplets of closely spaced lines. This is associated with the zero nuclear-spin of ^{16}O, which removes a set of lines usually visible for other systems, including the same Ar–O_2 complex but with the ^{17}O isotope. We anticipate that the predicted MW line positions should help narrow the search interval for future spectroscopic measurements.

The present procedure allows the generation of consistently accurate atom–atom and atom–molecule potentials by fitting available combinations of experimental parameters for specific complexes and by transferring the accuracy of such fits effectively to other related complexes: for instance, it is possible to determine RgX and RgY potentials either from fitting directly to experimental results characterizing the RgX and RgY complexes or from fitting to experimental results characterizing the Rg–X_2 and Rg–Y_2 complexes (depending upon the available and/or preferred experimental data) and then to make predictions for the Rg–XY complex.

This methodology can be extended to other cases (e.g. with more atom–diatom complexes involved simultaneously) or to employ also atom–triatom and larger species as objects for fitting [39]. In general, an arbitrary number of accurate atom–atom potentials can be determined from the same number of corresponding atom–molecule PESs, and then can be utilized to improve PESs for complexes consisting of other combinations of the same atoms. This therefore appears to provide a flexible means of transferring effective atom–atom components of intermolecular interactions.

This work was begun during FN's research associateship in the group of Professor F. R. W. McCourt and finalised during his visiting assistant professorship in the group of Professor J. C. Polanyi. FN is grateful to M. Wheeler (Leicester), I. McNab (Newcastle) and S. Dobrin (Toronto) for helpful discussions of the nuclear-spin issue. This work has been funded in part by an NSERC of Canada Discovery Grant.

References

[1] Pirani, F., and Vecchiocattivi, F., 1981, *Chem. Phys.*, **59,** 387.
[2] Candori, R., Pirani, F., and Vecchiocattivi, F., 1983, *Chem. Phys. Lett.*, **102,** 412.
[3] Gianturco, F. A., and Storozhev, A., 1994, *J. chem. Phys.*, **101,** 9624.
[4] van Lenthe, J. H., and van Duijneveldt, F. B., 1984, *J. chem. Phys.*, **81,** 3168.
[5] Jaquet, R., and Staemmler, V., 1986, *Chem. Phys.*, **101,** 243.
[6] Naumkin, F. Y., and Knowles, P. J., 1996, FEMTOCHEMISTRY—Ultrafast Chemical and Physical Processes in Molecular Systems, edited by M. Chergui (Singapore: World Scientific), p. 94.
[7] Naumkin, F. Y., and McCourt, F. R. W., 1997, *J. chem. Phys.*, **107,** 1185.
[8] Naumkin, F. Y., and McCourt, F. R. W., 1997, *J. chem. Phys.*, **107,** 5702.
[9] Cybulski, S. M., Kehdall, R. A., Chalasinski, G., Severson, M. W., and Szczesniak, M. M., 1997, *J. chem. Phys.*, **106,** 7731.
[10] Knowles, P. J., Hampel, C., and Werner, H.-J., 1993, *J. chem. Phys.*, **99,** 5219.
[11] Deegan, M. J. O., and Knowles, P. J., 1994, *Chem. Phys. Lett.*, **227,** 321.
[12] MOLPRO is a package of *ab initio* programs written by H.-J. Werner and P. J. Knowles, with contributions from J. Almlöf, R. D. Amos, A. Berning, M. J. O. Deegan, F. Eckert, S. T. Elbert, C. Hampel, R. Lindh, W. Meyer, A. Nicklass, K. Peterson, E.-A. Reinsch, R. M. Pitzer, A. J. Stone, P. R. Taylor, M. E. Mura, P. Pulay, M. Schuetz, H. Stoll, T. Thorsteinsson and D. L. Cooper.
[13] Kendall, R. A., Dunning Jr., T. H., and Harrison, R. J., 1992, *J. chem. Phys.*, **96,** 6796.
[14] Woon, D. E., and Dunning, T. H., 1993, *J. chem. Phys.*, **98,** 1358.
[15] Boys, S. F., and Bernardi, F., 1970, *Molec. Phys.*, **19,** 553.
[16] Naumkin, F. Y., 1999, *Phys. Chem. Chem. phys.*, **1,** 3949.
[17] Naumkin, F. Y., and McCourt, F. R. W., 1998, *J. chem. Phys.*, **109,** 1271.
[18] Tennyson, J., Miller, S., and LeSueur, C. R., 1993, *Comp. Phys. Commun.*, **75,** 339.
[19] Naumkin, F. Y., 1997, *Molec. Phys.*, **90,** 875.
[20] Buchachenko, A. A., Jakowski, J., Cybulski, S. M., Szczesniak, M. M., and Chalasinski, G., 2000, *J. chem. Phys.*, **112,** 5852.
[21] Aquilanti, V., Candori, R., and Pirani, F., 1988, *J. chem. Phys.*, **89,** 6157.
[22] Ma, Z., Liu, K., Harding, L. B., Komotos, M., and Schatz, G. C., 1994, *J. chem. Phys.*, **100,** 8026.
[23] Mills, P. D. A., Western, C. M., and Howard, B. J., 1986, *J. phys. Chem.*, **90,** 4961.
[24] Naumkin, F. Y., and McCourt, F. R. W., 1998, *J. chem. Phys.*, **108,** 9301.
[25] Feller, D., 1992, *J. chem. Phys.*, **96,** 6104.
[26] Helgaker, T., Klopper, W., Koch, H., and Noga, J., 1997, *J. chem. Phys.*, **106,** 9639.
[27] Petersen, K. A., and Dunning, T. H., 1997, *J. phys. Chem.*, **101,** 6280.
[28] Naumkin, F. Y., and Wales, D. J., 2000, *Molec. Phys.*, **98,** 219.
[29] Jaeger, W., Gerry, M. C. L., Bissonnette, C., and McCourt, F. R. W., 1994, *Faraday Discuss.*, **97,** 105.
[30] Fernandez, B., Koch, H., and Makarewicz, J., 1999, *J. chem. Phys.*, **110,** 8525.
[31] Alexander, M. H., 1999, *J. chem. Phys.*, **111,** 7435.
[32] Casavecchia, P., Lagana, A., and Volpi, G. G., 1984, *Chem. Phys. Lett.*, **112,** 445.

[33] MILLER, J. C., and CHENG, W.-C., 1985, *J. phys. Chem.*, **96**, 2573.
[34] MILLER, J. C., 1989, *J. chem. Phys.*, **90**, 4031.
[35] SCHMELZ, T., ROSMUS, P., and ALEXANDER, M. H., 1994, *J. phys. Chem.*, **98,** 1073.
[36] TSUJI, K., SHIBUYA, K., and OBI, K., 1994, *J. chem. Phys.*, **100,** 5441.
[37] STEINFELD, J. I., 1985, *Molecules and Radiation: an Introduction to Modern Molecular Spectroscopy* (Cambridge, MA: MIT Press), Ch. 4.1.
[38] HERZBERG, G., 1964, *Molecular Spectra and Molecular Structure*, Vol. 1, *Spectra of Diatomic Molecules* (Princeton, NJ: Van Nostrand).
[39] NAUMKIN, F. Y., 2004, to be published.